IJIE

INTERNATIONAL JOURNAL OF INTEGRATED ENGINEERING
ISSN: 2229-838X e-ISSN: 2600-7916

Vol. 18 No. 3 (2026) 118-134
https://publisher.uthm.edu.my/ojs/index.php/ijie

Proposed Double Sampling Variable Sampling Interval Coefficient of Variation Chart for Manufacturing

You Huay Woon[1], Michael Khoo Boon Chong[2]*, Sajal Saha[3], Yasar Mahmood[4], Shanyu Chua[5]

[1] *Pusat PERMATA@Pintar Negara, Universiti Kebangsaan Malaysia, 43600 Bangi, MALAYSIA*
[2] *School of Mathematical Sciences, Universiti Sains Malaysia, 11800 Penang, MALAYSIA*
[3] *Department of Mathematics, International University of Business Agriculture and Technology, Dhaka, BANGLADESH*
[4] *Department of Statistics, Government College University, Lahore, PAKISTAN*
[5] *Estek Automation Sdn Bhd, No. 53, Jalan Sungai Tiram 2, Nyaman Mutiara Light Industrial Park 2, Sungai Tiram, 11900 Bayan Lepas, Penang, MALAYSIA*

*Corresponding Author: mkbc@usm.my
DOI: https://doi.org/10.30880/ijie.2026.18.03.008

Article Info

Received: 5 September 2025
Accepted: 21 December 2025
Available online: 30 April 2026

Keywords

Statistical process control, variable sampling interval, coefficient of variation, double sampling, average time to signal

Abstract

The aim of this study is to develop a new control chart, known as the double sampling variable sampling interval coefficient of variation (DS VSI CV) chart for an improved monitoring of the process CV. Process monitoring in manufacturing usually requires the process mean or standard deviation to be controlled. Nevertheless, for many quality characteristics, their standard deviations change with their means. Under this situation, a coefficient of variation control chart is adopted to monitor the process. The double sampling scheme improves the Shewhart scheme in the detection of small and medium shifts. Also, varying the sampling interval can significantly improve a chart's sensitivity to identify process shifts. In this paper, the design of the double sampling chart by adopting a variable sampling interval scheme is suggested for controlling the coefficient of variation. Results are presented in the tables for the DS VSI CV chart. The DS VSI CV chart is compared with the DS CV, variable parameter coefficient of variation (VP CV), and exponentially weighted moving average coefficient of variation (EWMA CV) charts. From the comparison, the DS VSI CV chart surpasses the DS CV and VP CV charts in the detection of all sizes of shifts using the out-of-control average time to signal measure. Meanwhile, the EWMA CV chart beats the DS VSI CV chart for the sample size, $n_0 \geq 10$ and very small shift $\delta = 1.1$, for all in control CV, γ_0 values. For the out-of-control standard deviation of the time to signal criterion, the DS VSI CV chart overtakes the DS CV and VP CV charts for all (n_0, γ_0, δ) combinations. An example is provided to illustrate the application of the DS VSI CV chart to help quality engineers implement the proposed chart to monitor their manufacturing processes. This study contributes to a more effective scheme for the process CV, through the developed DS VSI CV chart that surpasses the existing CV charts' ability in detecting shifts in the process CV, making it a great tool in facilitating timely interventions to maintain process quality and efficiency.

1. Introduction

A control chart is a potent tool that is widely employed in statistical process monitoring in real-time to identify assignable causes for improving the quality of the products produced [20, 26]. In fact, process monitoring and diagnosing of the real issue is very important for quality improvement [14]. Process variation is divided into two categories; namely, chance and assignable causes. A process is under control when only chance causes exist and out-of-control when assignable causes exist. An out-of-control process is unstable, which causes non-conformance to specifications and resulting in the production of defective products [8].

Process monitoring procedure using control charts was proposed by Shewhart. Due to the ease and efficiency in monitoring and improving the process, control charts are extensively employed in various sectors [25]. The Shewhart chart was the earliest chart for controlling the mean, particularly for detecting medium to large process mean shifts. Since then, various research studies were carried out to enhance the detection ability of a Shewhart chart.

Many processes do not have the mean or standard deviation that is constant. Therefore, the usual mean or standard deviation type charts cannot be implemented to monitor the said processes. Under this situation, a typical relation is the proportionality of the standard deviation to the mean, whereby the standard deviation to the mean ratio remains constant. The said ratio is the coefficient of variation (CV). Consequently, control charts are developed for monitoring the CV to address situations when the mean and standard deviation type charts cannot be employed.

Various CV charts have been developed. Kang et al. [13] introduced the Shewhart CV chart. The Shewhart CV chart is slow in identifying small shifts. Hong et al. [9] developed the EWMA CV chart and evaluated the chart using simulation. Castagliola et al. [4] proposed runs rule (RR) type charts for CV monitoring, i.e. the 2-of-3, 3-of-4 and 4-of-5 schemes, and compared them with Shewhart CV chart. According to comparative results, the 2-of-3 and 4--of-5 schemes have better performance in most cases. Calzada and Scariano [3] introduced the synthetic CV chart, which combines the CV and conforming run length subcharts. Readers may refer to [5, 16, 18, 27], to name a few, for the recent works on CV charts.

The variable sampling interval (VSI) chart is an adaptive chart, where the sampling interval adopted in taking the next sample is varied according to the disposition of the previous sample. Compared to the traditional fixed sampling interval chart, the VSI chart exhibits superior sensitivity in detecting process shifts, where it is quicker in detecting small and moderate shifts. A key advantage of the VSI chart lies in its cost-effectiveness, as the chart strategically varies the sampling frequency, hence, reducing operational cost and maintaining robust monitoring capability [22]. A VSI chart's adaptability to fluctuating process conditions makes it particularly suitable in smart manufacturing environments, where rapid adjustments are critical in maintaining quality standards.

Numerous researchers had examined control charts with the VSI method. There are three regions in the VSI chart, i.e., (i) out-of-control, (ii) warning, and (iii) in-control. If a sample falls in the in-control region, then the next sample ought to be obtained after a long sampling interval because there is only a low probability that the process will become out-of-control. Nevertheless, if a sample plots in the warning region, then the next sample ought to be obtained after a short sampling interval to tighten control because the probability that the process goes out-of-control is high.

Yang et al. [23] introduced the VSI cumulative sum (VSI CUSUM) charts to monitor nutrient ratios in short production runs, showing their effectiveness in precision agriculture via dynamic sampling adjustments. Likewise, Zhang et al. [28] integrated the VSI-Tr charts with equipment maintenance strategies, optimizing cost-effectiveness in high-quality manufacturing, which reduces the expected cost per unit time by 15%. Hu et al. [10] extended the VSI method to develop the CUSUM multivariate CV charts using Markov chain derived parameters for monitoring shifts in the multivariate CV. For compositional data (CoDa) monitoring, Imran et al. [12] developed the VSI-MEWMA CoDa chart, leveraging isometric log-ratio transformation to reduce the detection times by 30% compared to using fixed sampling intervals. Tang et al. [19] concluded that their proposed nonparametric EWMA chart with VSI reduces the time taken to identify shifts than the competing charts developed using fixed sampling intervals. Teoh et al. [19] found that the VSI EWMA $\bar{X}$ chart needs many Phase-I samples to give satisfactory results. Some latest researches on VSI charts were conducted by [1, 2], to name a few.

Croasdale [6] pioneered the double sampling (DS) approach for identifying mean shifts. The DS technique from Croasdale [6] adopts the idea that an out-of-control situation only depends on the condition of the second sample and the first sample just indicates whether or not a second sample is required. Daudin [7] developed the DS chart through modification of the DS approach to include information from both first and second samples to identify the process state. Several studies have extended the DS procedure to increase the effectiveness of the basic DS scheme [15, 29]. Lee et al. [16] suggested the DS CV chart to control CV shifts. From the performance comparison, the DS CV chart beats the VP CV chart to detect all CV shift sizes. Meanwhile, the DS CV scheme performs better than the EWMA CV scheme by means of the ATS_1 criterion, except for very small shifts. Readers can consult [5, 17] for more insight on the DS and CV charts.

The DS VSI chart to monitor the process CV does not exist in the present literature. Despite advancements in CV monitoring using Shewhart, EWMA and synthetic charts, challenges persist in efficiently detecting small to moderate CV shifts, while striking a balance between sampling cost and operational complexity. While existing DS CV charts and VSI frameworks demonstrated improved sensitivity, the integration of DS with VSI for CV monitoring remains unexplored. Moreover, due to the rapidly evolving challenges in process monitoring, it is crucial to examine a relative measure of process variability, such as the CV, instead of using a single measure of the process parameter, particularly in manufacturing, to monitor process stability. The goal of this paper is to bridge this gap. This paper addresses this gap by proposing the DS VSI CV chart, aiming at increasing the detection speed of an out-of-control process CV, reducing sampling costs and enhancing adaptability in dynamic processes, where traditional mean or standard deviation charts are ineffective. By leveraging the synergistic benefits of the DS and VSI methods, this work seeks to advance CV monitoring methodologies, offering a robust solution for industries, which require high precision in quality control.

A performance measure of a control chart is crucial to assess the chart's effectiveness in detecting a process shift. A common performance measure is the average run length (ARL). The ARL is defined as the expected number of samples taken to detect the first out-of-control signal [24]. For situations where a control chart adopts varying sampling intervals in taking samples, such as the VSI type chart, the average time to signal (ATS) criterion, instead of the ARL is preferred. The ATS quantifies the actual average time taken to signal the first out-of-control condition, accounting for the variable sampling intervals between successive samples. In VSI schemes, such as the DS VSI CV chart, the sampling interval adopted to take the next sample is based on the process condition of the present sample, where a shorter interval is used when process deviations are suspected and a longer interval is used when the process is stable. The ARL measure is inadequate as it assumes fixed sampling intervals. Prior studies have validated ATS as the preferred measure for evaluating the performance of adaptive charts, such as the VSI type charts, as ATS aligns with operational priorities, for example cost reduction, rapid responses and resource optimization [21].

This paper is structured into several sections: The proposed DS VSI CV chart is enumerated in Section 2. The operation, as well as optimal design of the DS VSI CV chart are also enumerated in the same section. In Section 3, the computation of the optimal charting parameters of the DS VSI CV chart is discussed, and a comparison of the average time to signal (ATS) and standard deviation of the time to signal (SDTS) performances of the proposed DS VSI CV and existing DS CV, VP CV and EWMA CV charts is presented. A discussion on the novelty and shortcomings of the proposed DS VSI CV chart is also provided in Section 3. Section 4 shows the application of the DS VSI CV scheme. Finally, concluding remarks are given in Section 5.

2. A Proposed DS VSI CV Control Chart

Suppose that $\{X_1, X_2, \ldots, X_n\}$ are independent and identically distributed (iid) variables having the normal distribution, i.e., $X \sim N(\mu, \sigma^2)$. Also, assume that for an in-control process, σ is proportional to μ from one sample to the next, i.e., μ and σ can change but the ratio of σ to μ, defined as CV in Equation (1), is constant.

$$\gamma = \frac{\sigma}{\mu} \tag{1}$$

The sample CV is

$$\hat{\gamma} = \frac{S}{\bar{X}} \tag{2}$$

where $\bar{X}$ and S are computed as

$$\bar{X} = \frac{1}{n}\sum_{i=1}^{n} X_i \tag{3}$$

and

$$S = \sqrt{\frac{1}{n-1}\sum_{i=1}^{n}(X_i - \bar{X})^2} \tag{4}$$

respectively.

According to Iglewicz et al. [11], the sample CV has a non-central t distribution with n – 1 degrees of freedom and non-centraliy parameter $\sqrt{n}/\gamma$. It can be shown that the cumulative distribution function (cdf) of $\hat{\gamma}$ is

$$F_{\hat{\gamma}}(x|n,\gamma) = 1 - F_t\left(\frac{\sqrt{n}}{x}\middle|n-1,\frac{\sqrt{n}}{\gamma}\right) \tag{5}$$

with $F_t(\,.\,)$ being the non-central t cdf with n – 1 degrees of freedom and a non-centrality parameter $\sqrt{n}/\gamma$. Meanwhile, $\hat{\gamma}^2$ follows a non-central F distribution with (1, n – 1) degrees of freedom and a non-centrality parameter $\frac{n}{\gamma^2}$. Note that $\hat{\gamma}^2$ has the cdf

$$F_{\hat{\gamma}^2}(x|n,\gamma) = 1 - F_F\left(\frac{\sqrt{n}}{x}\middle|1,n-1,\frac{n}{\gamma^2}\right) \tag{6}$$

Note that $F_F(\,.\,)$ is the non-central F distribution with (1, n – 1) degrees of freedom and a non-centrality parameter $\frac{n}{\gamma^2}$.

A DS VSI CV chart includes the design parameters: n_1, n_2, h_1, h_2, UCL_1, LCL_1, UWL_2, LWL_2, UCL_2, LCL_2, UWL_1 and LWL_1. Here, UWL_2, LWL_2, UWL_1 and LWL_1 represent the warning limits that are used to decide on the sampling interval to be adopted. Note that UCL_1/LCL_1 are the DS VSI CV chart's upper/lower control limits for the first sampling stage and UCL_2/ LCL_2 are the chart's upper/lower control limits for the second sampling stage. Here, n_1 and n_2 denote the respective size of the samples taken at the first and second sampling stages of the DS VSI CV chart. Meanwhile, h_1/h_2 are the long/short sampling intervals. The DS VSI CV chart is displayed in Fig. 1 with the intervals: I_1 = [LWL_1, UWL_1], I_2 = [LWL_2, LWL_1] ∪ [UWL_1, UWL_2], I_3 = [LCL_1, LWL_2] ∪ [UWL_2, UCL_1] and I_4 = [LCL_2, UCL_2]. The warning and control limits are calculated using the following equations:

$$\mathrm{UCL}_i = \mu_0\left(\hat{\gamma}\middle|\textstyle\sum_{i=1}^{j} n_i\right) + ku_i\sigma_0\left(\hat{\gamma}\middle|\textstyle\sum_{i=1}^{j} n_i\right), \tag{7a}$$

$$\mathrm{LCL}_i = \mu_0\left(\hat{\gamma}\middle|\textstyle\sum_{i=1}^{j} n_i\right) - kl_i\sigma_0\left(\hat{\gamma}\middle|\textstyle\sum_{i=1}^{j} n_i\right), \tag{7b}$$

$$\mathrm{UWL}_2 = \mu_0(\hat{\gamma}|n_1) + wu_2\sigma_0(\hat{\gamma}|n_1), \tag{7c}$$

$$\mathrm{LWL}_2 = \mu_0(\hat{\gamma}|n_1) - wl_2\sigma_0(\hat{\gamma}|n_1), \tag{7d}$$

$$\mathrm{UWL}_1 = \mu_0(\hat{\gamma}|n_1) + wu_1\sigma_0(\hat{\gamma}|n_1), \tag{7e}$$

and

$$\mathrm{LWL}_1 = \mu_0(\hat{\gamma}|n_1) - wl_1\sigma_0(\hat{\gamma}|n_1) \tag{7f}$$

where j = 1 and 2 denote the first and second sampling stages, respectively. The $\mu_0(\,.\,)$ and $\sigma_0(\,.\,)$ in Equations (7a) – (7f) are computed by approximating the mean and standard deviation of $\hat{\gamma}$ [9] in Equations (8) and (9), respectively.

$$\mu_0\left(\hat{\gamma}\middle|\sum_{i=1}^{j} n_i\right) \simeq \gamma_0\left[1 + \frac{1}{\sum_{i=1}^{j} n_i}\left(\gamma_0^2 - \frac{1}{4}\right) + \frac{1}{\left(\sum_{i=1}^{j} n_i\right)^2}\left(3\gamma_0^4 - \frac{\gamma_0^2}{4} - \frac{7}{32}\right) + \frac{1}{\left(\sum_{i=1}^{j} n_i\right)^3}\left(15\gamma_0^6 - \frac{3\gamma_0^4}{4} - \frac{7\gamma_0^2}{32} - \frac{19}{128}\right)\right] \tag{8}$$

and

$$\sigma_0\left(\hat{\gamma}\left|\sum_{i=1}^{j} n_i\right.\right) \simeq \gamma_0\left[\frac{1}{\sum_{i=1}^{j} n_i}\left(\gamma_0^2+\frac{1}{2}\right)+\frac{1}{\left(\sum_{i=1}^{j} n_i\right)^2}\left(8\gamma_0^4+\gamma_0^2+\frac{3}{8}\right)+\frac{1}{\left(\sum_{i=1}^{j} n_i\right)^3}\left(69\gamma_0^6+\frac{7\gamma_0^4}{2}+\frac{3\gamma_0^2}{4}+\frac{3}{16}\right)\right]^{1/2} \tag{9}$$

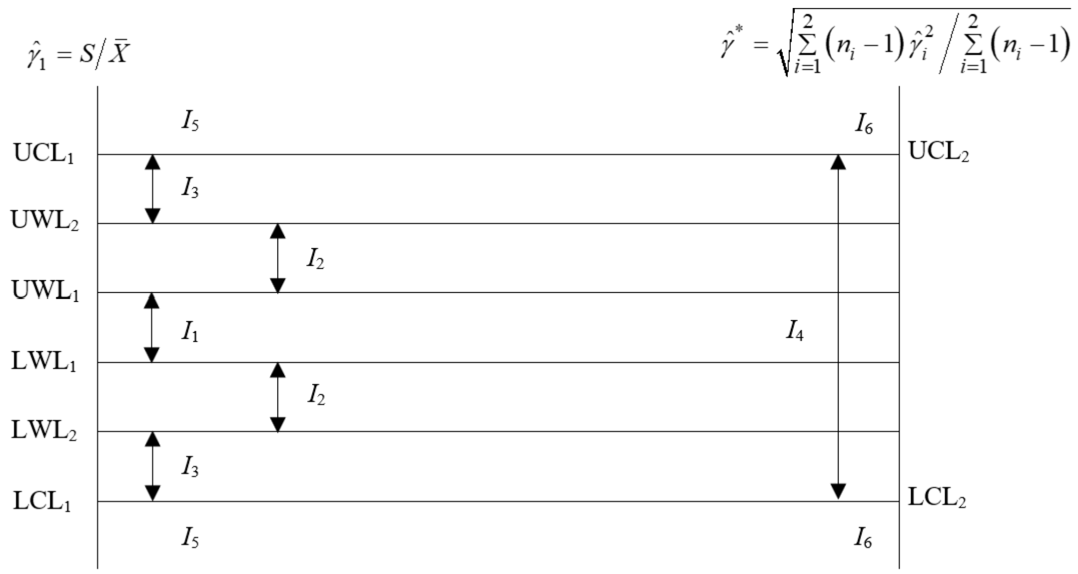

Fig. 1 *DS VSI CV chart*

The DS VSI CV scheme is established using two sampling stages. The first sample of size n_1 for the first sampling stage of the DS is plotted on the left scale using $\hat{\gamma}_1$ and the combined samples of size (n_1 + n_2) for the second sampling stage is plotted on the right scale based on $\hat{\gamma}^*$ (see Fig. 1). The DS VSI CV chart is implemented using the below steps:

(1) Select a sample with n_1 measurements, followed by computing the mean $\bar{X}_1$ and standard deviation S_1.
(2) Compute the sample CV, $\hat{\gamma}_1$ using Equation (2).
(3) If $\hat{\gamma}_1 \in I_1$, the long sampling interval, h_1, is adopted in taking the next sample.
(4) If $\hat{\gamma}_1 \in I_2$, the short sampling interval, h_2, is used in taking the next sample.
(5) If $\hat{\gamma}_1 \in I_5$, an out-of-control is signalled. Immediate action is performed to examine and eliminate the assignable cause(s).
(6) If $\hat{\gamma}_1 \in I_3$, take a second sample of size n_2 instantaneously. Then, the mean $\bar{X}_2$ and standard deviation S_2 are computed. Next, the sample CV, $\hat{\gamma}_2$ is calculated using Equation (2).
(7) Compute the combined sample CV, $\hat{\gamma}^* = \sqrt{\frac{\sum_{i=1}^{2}(n_i-1)\hat{\gamma}_i^2}{\sum_{i=1}^{2}(n_i-1)}}$.
(8) If $\hat{\gamma}^* \in I_4$, the process is in-control. Otherwise, an out-of-control is signalled and remedial action is needed to eliminate the assignable cause(s).

A process becomes out-of-control when the CV shifts from γ_0 (in-control CV) to γ_1 (out-of-control CV), where $\gamma_1 = \gamma_0 \times \delta$. Here, the process shift size can be obtained as $\delta = \frac{\gamma_1}{\gamma_0}$. The probability $\hat{\gamma}_1 \in I_5$ is

$$\begin{aligned} P(\hat{\gamma}_1 \in I_5 | \gamma_1 = \gamma_0 \times \delta) &= 1 - P(\mathrm{LCL}_1 \le \hat{\gamma}_1 \le \mathrm{UCL}_1 | n_1, \gamma_1 = \gamma_0 \times \delta) \\ &= 1 - F_{\hat{\gamma}}(\mathrm{UCL}_1 | n_1, \gamma_1) + F_{\hat{\gamma}}(\mathrm{LCL}_1 | n_1, \gamma_1) \end{aligned} \tag{10}$$

Meanwhile, the probability $\hat{\gamma}_1 \in I_3$ is

$$\begin{aligned} P(\hat{\gamma}_1 \in I_3 | \gamma_1 = \gamma_0 \times \delta) = {} & P(\mathrm{LCL}_1 \le \hat{\gamma}_1 \le \mathrm{LWL}_2 | n_1, \gamma_1 = \gamma_0 \times \delta) + \\ & P(\mathrm{UWL}_2 \le \hat{\gamma}_1 \le \mathrm{UCL}_1 | n_1, \gamma_1 = \gamma_0 \times \delta) \end{aligned} \tag{11}$$

Using the density function of non-central t distribution, $f_t(.)$, with n – 1 degree of freedom and a non-centrality parameter $\frac{\sqrt{n}}{\gamma}$, Equation (11) becomes

$$P(\hat{\gamma}_1 \in I_3 | \gamma_1 = \gamma_0 \times \delta) = \int_{\frac{\sqrt{n_1}}{\mathrm{LWL}_2}}^{\frac{\sqrt{n_1}}{\mathrm{LCL}_1}} f_t\left(u_1 \middle| n_1 - 1, \frac{\sqrt{n_1}}{\gamma_1}\right) du_1 + \int_{\frac{\sqrt{n_1}}{\mathrm{UCL}_1}}^{\frac{\sqrt{n_1}}{\mathrm{UWL}_2}} f_t\left(u_1 \middle| n_1 - 1, \frac{\sqrt{n_1}}{\gamma_1}\right) du_1 \tag{12}$$

In Equation (12), u_1 has the form

$$u_1 = \frac{\sqrt{n_1}}{\hat{\gamma}_1} \tag{13}$$

As the DS VSI CV chart involves two sampling stages, the probability that $\hat{\gamma}^*$ falls in the interval outside of [LCL$_2$, UCL$_2$], i.e. I_6, is

$$\begin{aligned} P\left(\hat{\gamma}^* \in I_6 \middle| \sum_{i=1}^{2} n_i, \gamma_1 = \gamma_0 \times \delta\right) &= 1 - P\left(\hat{\gamma}^* \in I_4 \middle| \sum_{i=1}^{2} n_i, \gamma_1\right) \\ &= 1 - P\left(\mathrm{LCL}_2 \le \hat{\gamma}^* \le \mathrm{UCL}_2 \middle| \sum_{i=1}^{2} n_i, \gamma_1\right) \end{aligned} \tag{14}$$

As $\hat{\gamma}^* = \sqrt{\frac{\sum_{i=1}^{2}(n_i-1)\hat{\gamma}_i^2}{\sum_{i=1}^{2}(n_i-1)}}$, Equation (14) becomes

$$P\left(\hat{\gamma}^* \in I_6 \middle| \sum_{i=1}^{2} n_i, \gamma_1 = \gamma_0 \times \delta\right) = 1 - P\left(\mathrm{LCL}_2^2 \le \frac{(n_1-1)\hat{\gamma}_1^2 + (n_2-1)\hat{\gamma}_2^2}{(n_1-1)+(n_2-1)} \le \mathrm{UCL}_2^2 \middle| \sum_{i=1}^{2} n_i, \gamma_1\right) \tag{15}$$

With some simplifications, Equation (15) reduces to

$$\begin{aligned} P\left(\hat{\gamma}^* \in I_6 \middle| \sum_{i=1}^{2} n_i, \gamma_1 = \gamma_0 \times \delta\right) &= 1 - P\left[\left(\frac{n_1-1}{n_2-1} + 1\right)(\mathrm{LCL}_2^2) - \frac{n_1-1}{n_2-1}\hat{\gamma}_1^2 \le \hat{\gamma}_2^2\right. \\ &\left.\le \left(\tfrac{n_1-1}{n_2-1} + 1\right)(\mathrm{UCL}_2^2) - \tfrac{n_1-1}{n_2-1}\hat{\gamma}_1^2 \middle| \textstyle\sum_{i=1}^{2} n_i, \gamma_1\right]. \end{aligned} \tag{16}$$

Equation (13) can be expressed as

$$\hat{\gamma}_1 = \frac{\sqrt{n_1}}{u_1} \tag{17}$$

By substituting Equation (17) into Equation (16), Equation (16) becomes

$$\begin{aligned} P\left(\hat{\gamma}^* \in I_6 \middle| \sum_{i=1}^{2} n_i, \gamma_1 = \gamma_0 \times \delta\right) &= 1 - P\left[\left(\frac{n_1-1}{n_2-1} + 1\right)(\mathrm{LCL}_2^2) - \frac{(n_1-1)n_1}{(n_2-1)u_1^2} \le \hat{\gamma}_2^2\right. \\ &\left.\le \left(\frac{n_1-1}{n_2-1} + 1\right)(\mathrm{UCL}_2^2) - \frac{(n_1-1)n_1}{(n_2-1)u_1^2} \middle| \sum_{i=1}^{2} n_i, \gamma_1\right] \end{aligned} \tag{18}$$

Let $\mathrm{LCL}_2^\dagger$ and $\mathrm{UCL}_2^\dagger$ be

$$\mathrm{LCL}_2^\dagger = \left(\frac{n_1-1}{n_2-1} + 1\right)(\mathrm{LCL}_2^2) - \frac{n_1(n_1-1)}{(n_2-1)u_1^2} \tag{19a}$$

and

$$\mathrm{UCL}_2^{\dagger}=\left(\frac{n_1-1}{n_2-1}+1\right)\left(\mathrm{UCL}_2^2\right)-\frac{n_1(n_1-1)}{(n_2-1)u_1^2}, \tag{19b}$$

respectively. Then, Equation (18) can be rewritten as

$$P\left(\hat{\gamma}^*\in I_6\left|\sum_{i=1}^{2}n_i,\gamma_1=\gamma_0\times\delta\right.\right)=1-P\left(\mathrm{LCL}_2^{\dagger}\le\hat{\gamma}_2^2\le\mathrm{UCL}_2^{\dagger}\left|\sum_{i=1}^{2}n_i,\gamma_1\right.\right) \tag{20}$$

Using the cdf of $\hat{\gamma}^2$ in Equation (6), Equation (20) becomes

$$P(\hat{\gamma}^*\in I_6|\textstyle\sum_{i=1}^{2}n_i,\gamma_1=\gamma_0\times\delta)=1-F_{\hat{\gamma}^2}\left(\mathrm{UCL}_2^{\dagger}|n_2,\gamma_1\right)+F_{\hat{\gamma}^2}\left(\mathrm{LCL}_2^{\dagger}|n_2,\gamma_1\right) \tag{21}$$

The probability $\hat{\gamma}_1\in I_3$ and $\hat{\gamma}^*\in I_6$, i.e., $P(\hat{\gamma}_1\in I_3\cap\hat{\gamma}^*\in I_6|\gamma_1=\gamma_0\times\delta)$ is

$$\int_{\frac{\sqrt{n_1}}{\mathrm{LWL}_2}}^{\frac{\sqrt{n_1}}{\mathrm{LCL}_1}}\left[1-F_{\hat{\gamma}^2}\left(\mathrm{UCL}_2^{\dagger}|n_2,\gamma_1\right)+F_{\hat{\gamma}^2}\left(\mathrm{LCL}_2^{\dagger}|n_2,\gamma_1\right)\right]\times f_t\left(u_1\left|n_1-1,\frac{\sqrt{n_1}}{\gamma_1}\right.\right)du_1+$$
$$\int_{\frac{\sqrt{n_1}}{\mathrm{UCL}_1}}^{\frac{\sqrt{n_1}}{\mathrm{UWL}_2}}\left[1-F_{\hat{\gamma}^2}\left(\mathrm{UCL}_2^{\dagger}|n_2,\gamma_1\right)+F_{\hat{\gamma}^2}\left(\mathrm{LCL}_2^{\dagger}|n_2,\gamma_1\right)\right]\times f_t\left(u_1\left|n_1-1,\frac{\sqrt{n_1}}{\gamma_1}\right.\right)du_1 \tag{22}$$

The probability for a process being out-of-control on the DS VSI CV chart for the shift size, δ is

$$P_{\mathrm{OOC}}=P(\hat{\gamma}_1\in I_5|\gamma_1=\gamma_0\times\delta)+P(\hat{\gamma}_1\in I_3\cap\hat{\gamma}^*\in I_6|\gamma_1=\gamma_0\times\delta), \tag{23}$$

where $P(\hat{\gamma}_1\in I_5|\gamma_1=\gamma_0\times\delta)$ and $P(\hat{\gamma}_1\in I_3\cap\hat{\gamma}^*\in I_6|\gamma_1=\gamma_0\times\delta)$ are given in Equations (10) and (22), respectively. From Equation (23), the average run length (ARL) and standard deviation of the run length (SDRL) for the shift size δ are

$$\mathrm{ARL}=\frac{1}{P_{\mathrm{ooc}}} \tag{24}$$

and

$$\mathrm{SDRL}=\frac{\sqrt{1-P_{\mathrm{OOC}}}}{P_{\mathrm{OOC}}}, \tag{25}$$

respectively. The average sample size (ASS) can be calculated using Equation (26).

$$\mathrm{ASS}=n_1+n_2\times P(\hat{\gamma}_1\in I_3|\gamma_1=\gamma_0\times\delta) \tag{26}$$

By using the cdf of $\hat{\gamma}$ in Equation (5), Equation (26) becomes

$$\mathrm{ASS}=n_1+n_2\times\left[F_{\hat{\gamma}}(\mathrm{UCL}_1|n_1,\gamma_1)-F_{\hat{\gamma}}(\mathrm{LCL}_1|n_1,\gamma_1)-F_{\hat{\gamma}}(\mathrm{UWL}_2|n_1,\gamma_1)+F_{\hat{\gamma}}(\mathrm{LWL}_2|n_1,\gamma_1)\right]. \tag{27}$$

Since the DS VSI CV chart adopts the sampling interval based on where $\hat{\gamma}_1$ plots on the DS chart, the ATS and SDTS are employed in evaluating the chart and are defined in Equations (28) and (29), respectively.

$$\mathrm{ATS}=\mathrm{ARL}\times\left[h_2\times\left(1-\frac{P(I_1)}{1-P_{\mathrm{OOC}}}\right)+h_1\times\left(\frac{P(I_1)}{1-P_{\mathrm{OOC}}}\right)\right] \tag{28}$$

and

$$\mathrm{SDTS}=\mathrm{SDRL}\times\left[h_2\times\left(1-\frac{P(I_1)}{1-P_{\mathrm{OOC}}}\right)+h_1\times\left(\frac{P(I_1)}{1-P_{\mathrm{OOC}}}\right)\right] \tag{29}$$

The optimal charting parameters of the DS VSI CV chart are determined using the following optimization model:

Minimize ATS_1, (30a)

subject to $\text{ATS}_0 = 370.4$ (30b)

and

$\text{ASS}_0 = n_0$, (30c)

where n_0 is the fixed sample size of the basic CV chart, while $\text{ATS}_0/\text{ATS}_1$ are the in-control/out-of-control ATS and ASS_0 is the in-control ASS.

The computational procedure to compute the optimal parameters $(n_1, n_2, ku_1, kl_1, wu_2, wl_2, ku_2, kl_2, wu_1, wl_1)$ of the DS VSI CV chart is as follows:

(1) Specify n_0, δ, h_1, h_2 ($h_1 > h_2$) and ATS_0, where δ is the size of CV shift which must be detected quickly, and n_0 is the fixed sample size of the basic CV scheme.
(2) Set trial values of n_1 and n_2 using the constraints n_1 = 2 to n_0 – 1 and n_2 = 2 to $5n_0$, and $n_1 + n_2 > n_0$.
(3) Initialize ku_1, kl_1 and wl_2, and compute wu_2 to satisfy the in-control ASS (ASS_0).
(4) Initialize kl_2 and compute ku_2 to satisfy the DS VSI CV chart's in-control ATS (ATS_0) value.
(5) Initialize wl_1 and compute wu_1 to satisfy the ATS_0 specified in Step 1, based on the parameter combination $(n_1, n_2, h_1, h_2, ku_1, kl_1, wu_2, wl_2, ku_2, kl_2)$ set or computed in prior steps.
(6) Compute ATS_1 based on $(n_1, n_2, h_1, h_2, ku_1, kl_1, wu_2, wl_2, ku_2, kl_2, wu_1, wl_1)$.

3. Performance Comparison and Discussion

In this section, the optimal parameters and limits of the DS VSI CV chart are calculated to minimize ATS_1 when $\text{ATS}_0 = 370.4$. Lee et al. [16] compared the DS CV, VP CV and EWMA CV schemes. It was concluded that the DS CV scheme beats the VP CV scheme. Nevertheless, the EWMA CV scheme outperforms the DS CV scheme in the detection of small shifts, regardless of the n_0 and γ_0 values. Therefore, the DS VSI CV chart's performance is compared with that of the DS CV, VP CV and EWMA CV charts. Note that $\delta \in (0,1)$ and $\delta > 1$ represent a downward and an upward CV shift, respectively. An upward shift in the CV suggests an increase in the process standard deviation relative to the process mean, whereas a downward shift in the CV reflects the opposite. An increasing standard deviation in the process monitored signals a deteriorating process, which is unwanted. In contrast, a decreasing standard deviation indicates process improvement. This demonstrates that monitoring an upward CV shift is more important than monitoring a downward one. Therefore, an upward CV shift, $\delta \in \{1.1, 1.2, 1.5, 2.0\}$ is considered here. In addition, various combinations of the sample size, $n_0 \in \{5, 10, 15\}$ and in-control CV, $\gamma_0 \in \{0.05, 0.1\}$ are taken into account for an equal footing comparison with those of other charts. Since the proposed chart is a VSI-type chart, therefore, sampling intervals h_1 = 1.9 (long) and h_2 = 0.1 (short) are used.

Table 1 displays the optimal charting parameters of DS VSI CV chart. In Table 1, it may appear that as n_0 increases, both n_1 and n_2 also increase, except when n_0 = 10, $\gamma_0 = 0.05$ and $\delta = 1.2$. For this case, the n_1 and n_2 values are 3 and 27, respectively. In addition, the value of n_1 decreases or remains the same when δ increases and $n_0 \in \{10,15\}$, regardless of the value of γ_0. For instance, when n_0 = 10, $\gamma_0 = 0.1$ and $\delta = 1.1$, n_1 = 8 compared to n_1 = 6 for the fixed n_0 and γ_0 values with δ increases to $\delta = 1.2$. It is also noted that ku_1 is always equal to 5. The range for kl_1 is [1.9, 2.3], [1.9, 3.2] and [3.5, 3.6] for n_0 = 5, 10 and 15, respectively. Nonetheless, there is no specific trend observed for kl_1, wu_2, wl_2, ku_2, kl_2, wu_1 and wl_1. Table 2 gives the optimal limits for the DS VSI CV chart obtained from Equations (7a) – (7f) by employing the optimal parameters from Table 1.

Table 1 *Optimal charting parameters of DS VSI CV chart when* $\boldsymbol{n_0} \in \{\mathbf{5}, \mathbf{10}, \mathbf{15}\}$*,* $\boldsymbol{\gamma_0} \in \{\mathbf{0.05}, \mathbf{0.1}\}$*,* $\boldsymbol{\delta} \in \{\mathbf{1.1}, \mathbf{1.2}, \mathbf{1.5}, \mathbf{2.0}\}$*, sampling intervals h1 = 1.9 and h2 = 0.1, based on minimizing* $\mathbf{ATS_1}$ *when* $\mathbf{ATS_0} = \mathbf{370.4}$

n_0	γ_0	δ	n_1	n_2	ku_1	kl_1	wu_2	wl_2	ku_2	kl_2	wu_1	wl_1
5	0.05	1.1	3	25	5	1.9	0.6494	1.000	2.7832	4.300	0.4375	0.9
		1.2	3	21	5	1.9	0.5933	1.000	2.8247	4.100	0.4375	0.9
		1.5	3	20	5	1.9	0.8105	1.200	2.7783	3.900	0.2344	1.1
		2.0	3	20	5	1.9	1.3379	1.800	2.6050	4.700	0.0211	1.4
	0.1	1.1	4	20	5	2.3	0.7764	1.000	2.8516	3.700	0.4375	0.9
		1.2	4	20	5	2.2	0.7764	1.000	2.8931	4.100	0.4375	0.9
		1.5	4	20	5	2.3	1.2500	1.400	2.7246	3.700	0.1203	1.3
		2.0	4	20	5	2.2	1.7676	2.100	2.5879	3.400	0.0246	1.5
10	0.05	1.1	7	26	5	3.2	1.2256	3.045	2.7197	3.028	0.0059	1.8
		1.2	3	27	5	1.9	0.1758	1.100	2.8467	4.100	0.3266	1.0
		1.5	6	26	5	2.3	0.9473	1.900	3.4570	3.800	0.0074	1.7
		2.0	6	26	5	2.3	0.9888	2.100	3.4473	3.700	0.0082	1.7
	0.1	1.1	8	26	5	3.0	1.1914	1.600	2.7710	4.000	0.0875	1.5
		1.2	6	26	5	3.0	0.9302	1.800	2.7832	3.600	0.0070	1.7
		1.5	6	26	5	3.0	0.9302	1.800	2.7832	3.600	0.0070	1.7
		2.0	6	26	5	3.0	1.0254	2.500	2.7588	4.500	0.0098	1.7
15	0.05	1.1	10	29	5	3.5	0.9448	3.400	2.8052	3.200	0.0066	1.9
		1.2	8	28	5	3.5	0.6519	3.400	2.8345	3.200	0.0133	1.8
		1.5	8	28	5	3.6	0.6519	3.400	2.8345	3.200	0.0133	1.8
		2.0	8	28	5	3.6	0.6519	3.400	2.8345	4.000	0.0133	1.8
	0.1	1.1	10	29	5	3.5	0.9424	3.400	2.8174	3.300	0.0033	1.9
		1.2	8	28	5	3.5	0.6494	3.400	2.8467	3.300	0.0133	1.8
		1.5	8	28	5	3.6	0.6494	3.400	2.8467	4.000	0.0133	1.8
		2.0	8	30	5	3.5	0.7080	3.400	2.8271	4.100	0.0066	1.8

Table 2 indicates that UCL_1 is the same for n_0 = 5 when $\gamma_0 = 0.05$ and $\gamma_0 = 0.1$, i.e., 0.1607 and 0.2890, respectively, regardless of δ. Besides, the LCL_1 increases when n_0 increases from 5 to 10, except when n_0 = 10, $(\gamma_0, \delta) \in \{(0.05, 1.2), (0.1, 1.2), (0.1, 2.0)\}$. For example, when n_0 = 5, $\gamma_0 = 0.1$ and δ = 1.1, the LCL_1 = 0.0019. When n_0 increases to 10 for the same γ_0 and δ values, the LCL_1 becomes 0.0172. For the fixed n_0 and δ values, when γ_0 increases from 0.05 to 0.1, the UWL_2, LWL_2, UCL_2, LCL_2, UWL_1, LWL_1 generally also increase. For instance, when n_0 = 15, $\gamma_0 = 0.05$ and δ = 1.2, the corresponding UWL_2 = 0.0568, LWL_2 = 0.0036, UCL_2 = 0.0666, LCL_2 = 0.0305, UWL_1 = 0.0484 and LWL_1 = 0.0246, are optimally obtained by minimizing ATS_1, when $\text{ATS}_0 = 370.4$. However, when γ_0 increases to 0.1 and for the same n_0 and δ values, UWL_2 = 0.1138, LWL_2 = 0.0066, UCL_2 = 0.1336, LCL_2 = 0.0596, UWL_1 = 0.0970, LWL_1 = 0.0489 are attained.

Table 2 *Control limits of DS VSI CV chart when* $\boldsymbol{n_0} \in \{\mathbf{5, 10, 15}\}$, $\boldsymbol{\gamma_0} \in \{\mathbf{0.05, 0.1}\}$, $\boldsymbol{\delta} \in \{\mathbf{1.1, 1.2, 1.5, 2.0}\}$, *sampling intervals h1 = 1.9 and h2 = 0.1, based on minimizing* $\mathbf{ATS_1}$ *when* $\mathbf{ATS_0} = \mathbf{370.4}$

n_0	γ_0	δ	n_1	n_2	UCL_1	LCL_1	UWL_2	LWL_2	UCL_2	LCL_2	UWL_1	LWL_1
5	0.05	1.1	3	25	0.1607	0.0002	0.0595	0.0211	0.0684	0.0204	0.0546	0.0234
		1.2	3	21	0.1607	0.0002	0.0582	0.0211	0.0702	0.0193	0.0546	0.0234
		1.5	3	20	0.1607	0.0002	0.0632	0.0165	0.0703	0.0201	0.0498	0.0188
		2.0	3	20	0.1607	0.0002	0.0755	0.0025	0.0690	0.0141	0.0449	0.0118
	0.1	1.1	4	20	0.2890	0.0019	0.1229	0.0531	0.1412	0.0442	0.1096	0.0570
		1.2	4	20	0.2890	0.0059	0.1229	0.0531	0.1418	0.0382	0.1096	0.0570
		1.5	4	20	0.2890	0.0019	0.1415	0.0373	0.1393	0.0442	0.0971	0.0413
		2.0	4	20	0.2890	0.0059	0.1619	0.0098	0.1373	0.0486	0.0934	0.0334
10	0.05	1.1	7	26	0.1187	0.0027	0.0653	0.0049	0.0666	0.0307	0.0481	0.0225
		1.2	3	27	0.1607	0.0002	0.0485	0.0188	0.0682	0.0227	0.0520	0.0211
		1.5	6	26	0.1247	0.0121	0.0622	0.0183	0.0715	0.0255	0.0477	0.0214
		2.0	6	26	0.1247	0.0121	0.0628	0.0152	0.0715	0.0261	0.0477	0.0214
	0.1	1.1	8	26	0.2291	0.0172	0.1282	0.0542	0.1336	0.0497	0.0989	0.0569
		1.2	6	26	0.2507	0.0021	0.1242	0.0394	0.1348	0.0532	0.0955	0.0425
		1.5	6	26	0.2507	0.0021	0.1242	0.0394	0.1348	0.0532	0.0955	0.2507
		2.0	6	26	0.2507	0.0021	0.1272	0.0176	0.1345	0.0417	0.0956	0.0425
15	0.05	1.1	10	29	0.1069	0.0079	0.0596	0.0091	0.0658	0.0313	0.0487	0.0265
		1.2	8	28	0.1140	0.0023	0.0568	0.0036	0.0666	0.0305	0.0484	0.0246
		1.5	8	28	0.1140	0.0010	0.0568	0.0036	0.0666	0.0305	0.0484	0.0246
		2.0	8	28	0.1140	0.0010	0.0568	0.0036	0.0666	0.0258	0.0484	0.0246
	0.1	1.1	10	29	0.2147	0.0152	0.1195	0.0176	0.1319	0.0613	0.0974	0.0528
		1.2	8	28	0.2291	0.0039	0.1138	0.0066	0.1336	0.0596	0.0970	0.0489
		1.5	8	28	0.2291	0.0013	0.1138	0.0066	0.1336	0.0512	0.0970	0.0489
		2.0	8	30	0.2291	0.0039	0.1154	0.0066	0.1324	0.0514	0.0968	0.0489

Tables 3 and 4 give ATS_1s and $SDTS_1$s of DS VSI CV, DS CV, VP CV and EWMA CV charts, respectively, for different combinations of $n_0 \in \{5, 10, 15\}$, $\gamma_0 \in \{0.05, 0.1\}$ and $\delta \in \{1.1, 1.2, 1.5, 2.0\}$ (i.e., increasing CV shifts). The ATS_1s and $SDTS_1$s of the DS VSI CV chart are computed by employing the optimal parameters from Table 1. For illustration, when n_0 = 5, h_1 = 1.9, h_2 = 0.1, $\gamma_0 = 0.05$ and $\delta = 1.1$, the corresponding optimal parameters that are computed by minimizing ATS_1 when $ATS_0 = 370.4$ are n_1 = 3, n_2 = 25, ku_1 = 5, kl_1 = 1.9, wu_2 = 0.6494, wl_2 = 1.000, ku_2 = 2.7832, kl_2 = 4.300, wu_1 = 0.4375 and wl_1 = 0.9 (see Table 1). Using these optimal charting parameters, the ATS_1 and $SDTS_1$ of the DS VSI CV chart are 42.93 (see Table 3) and 42.46 (see Table 4), respectively. For this particular (n_0, γ_0, δ) combination, the ATS_1 value for the DS CV, VP CV and EWMA CV charts are 56.33, 84.11 and 52.21, respectively (see Table 3). By setting the same ATS_0 for all the charts under comparison, the chart that gives the smallest ATS_1 for a given size of shift is considered more efficient than its competitors. This demonstrates that the DS VSI CV chart surpasses the DS CV, VP CV and EWMA CV charts. The comparison shows that the DS VSI CV chart is superior to the competing charts by 17.77% to 48.96% (see Table 3). For the $SDTS_1$ criterion with the same (n_0, γ_0, δ) combination, the DS VSI CV chart prevails over the DS CV and VP CV charts by 23.95% and 43.72%, respectively, but the EWMA CV chart beats the DS VSI CV chart by 0.30%. A 0.30% difference in the performance of both the charts can be considered as insignificant. The associated optimal sample sizes, control and warning limits at the first and second sampling stages when n_0 = 5, h_1 = 1.9, h_2 = 0.1, $\gamma_0 = 0.05$ and $\delta = 1.1$ are (n_1, n_2, UCL_1, LCL_1, UWL_2, LWL_2, UCL_2, LCL_2, UWL_1, LWL_1) = (3, 25, 0.1607, 0.0002, 0.0595, 0.0211, 0.0684, 0.0204, 0.0546, 0.0234) (see Table 2).

Table 3 $\mathbf{ATS_1 s}$ *for DS VSI CV, DS CV, VP CV and EWMA CV charts for* $\boldsymbol{n_0} \in \{\mathbf{5,10,15}\}$, $\boldsymbol{\gamma_0} \in \{\mathbf{0.05, 0.1}\}$ *and* $\boldsymbol{\delta} \in \{\mathbf{1.1, 1.2, 1.5, 2.0}\}$, *based on minimizing* $\mathbf{ATS_1}$ *when* $\mathbf{ATS_0} = \mathbf{370.4}$

n_0	γ_0	δ	DS VSI CV	DS CV	VP CV	EWMA CV
5	0.05	1.1	42.93	56.33 (23.79%)[1]	84.11 (48.96%)	52.21 (17.77%)
		1.2	12.53	17.08 (26.64%)	21.56 (41.88%)	20.95 (40.19%)
		1.5	2.56	3.51 (26.78%)	4.65 (44.73%)	6.72 (61.76%)
		2.0	1.41	1.85 (23.78%)	2.38 (40.76%)	3.09 (54.37%)
	0.1	1.1	46.84	56.83 (17.58%)	91.97 (49.07%)	52.51 (10.80%)
		1.2	12.59	17.31 (27.29%)	23.90 (47.34%)	21.22 (40.69%)
		1.5	2.13	3.55 (40.00%)	4.37 (51.26%)	6.83 (68.81%)
		2.0	1.00	1.86 (46.24%)	2.26 (55.75%)	3.14 (68.15%)
10	0.05	1.1	32.65	38.77 (15.79%)	63.38 (48.49%)	30.98 (-5.39%)
		1.2	9.36	9.95 (5.93%)	12.00 (22.00%)	12.25 (23.59%)
		1.5	1.32	1.90 (30.53%)	2.18 (39.45%)	4.12 (67.96%)
		2.0	0.79	1.18 (33.05%)	1.43 (44.76%)	1.99 (60.30%)
	0.1	1.1	31.69	39.24 (19.24%)	68.24 (53.56%)	31.30 (-1.25%)
		1.2	7.40	10.12 (26.88%)	13.31 (44.40%)	12.40 (40.32%)
		1.5	1.29	1.93 (33.16%)	2.07 (37.68%)	4.17 (69.06%)
		2.0	0.80	1.19 (32.77%)	1.32 (39.39%)	2.01 (60.20%)
15	0.05	1.1	24.73	31.71 (22.01%)	56.12 (55.93%)	22.95 (-7.76%)
		1.2	5.34	7.56 (29.37%)	9.00 (40.67%)	9.06 (41.06%)
		1.5	1.01	1.48 (31.76%)	1.48 (31.76%)	3.12 (67.63%)
		2.0	0.87	1.06 (17.93%)	1.10 (20.91%)	1.56 (44.23%)
	0.1	1.1	25.11	32.11 (21.80%)	57.05 (55.99%)	23.23 (-8.09%)
		1.2	5.47	7.69 (28.87%)	9.24 (40.80%)	9.17 (40.35%)
		1.5	1.02	1.49 (31.54%)	1.49 (31.54%)	3.16 (67.72%)
		2.0	0.82	1.06 (22.64%)	1.11 (26.13%)	1.58 (48.10%)

The entries in the parentheses represent the percentage of improvement in the DS VSI CV chart compared to the competing charts.

A comparison of the ATS_1 performance with the DS CV and VP CV charts indicates the superiority of the DS VSI CV chart for all (n_0, γ_0 δ) combinations, as the latter has the smallest ATS_1 value for identifying a specific shift magnitude δ. The detection ability of the DS VSI CV chart is better than that of the DS CV and VP CV charts by 5.93% to 46.24% and 20.91% to 55.99%, respectively (see Table 3). For example, when $n_0 = 5$, $\gamma_0 = 0.1$ and $\delta = 1.2$, the ATS_1 value for the DS VSI CV, DS CV and VP CV charts are 12.59, 17.31 and 23.90, respectively. From this comparison, the DS VSI CV chart has the quickest response when $\delta = 1.2$ as it provides the lowest ATS_1 value (= 12.59). Hence, the DS VSI CV chart is the most efficient chart for $n_0 = 5$, $\gamma_0 = 0.1$ and $\delta = 1.2$ combination. Nevertheless, the EWMA CV chart beats the other charts when δ is approaching unity, i.e., $\delta = 1.1$ and $n_0 \geq 10$ for $\gamma_0 \in \{0.05, 0.1\}$. For example, when $n_0 = 10$, $\gamma_0 = 0.05$ and $\delta = 1.1$, the ATS_1 value for the EWMA CV chart is 30.98. For the same settings, the DS VSI CV, DS CV and VP CV charts' ATS_1s are 32.65, 38.77 and 63.38, respectively. By having the lowest ATS_1 value, the EWMA CV chart is superior to the other charts. Furthermore, the EWMA CV chart outperforms the DS VSI CV chart by 5.39%, for this (n_0, γ_0 δ) combination. The EWMA CV chart generally surpasses the DS VSI CV chart by 1.25% to 8.09%. However, the DS VSI CV chart overtakes the EWMA CV chart when $n_0 = 5$ (for $\delta \in \{1.1,1.2,1.5,2.0\}$) and $n_0 \geq 10$ (for $\delta \in \{1.2,1.5,2.0\}$), regardless of γ_0.

For the SDTS_1 performance, the DS VSI CV chart outclasses the DS CV and VP CV charts for all (n_0, γ_0 δ) combinations. On the contrary, the EWMA CV chart provides the best performance among all the charts when $n_0 = 5$ (for $\delta = 1.1$) and $n_0 \in \{10, 15\}$ (for $\delta \in \{1.1,1.2\}$), for all γ_0 values (see Table 4). The DS VSI CV chart comes in second place for these (n_0, γ_0, δ) combinations. In general, the EWMA CV chart exhibits the lowest SDTS_1 values for small shift sizes when compared to the other charts. As an example, when $n_0 = 5$, the EWMA CV chart performs best for $\gamma_0 \in \{0.05, 0.1\}$ and $\delta = 1.1$ with $\text{SDTS}_1 \in \{42.33, 42.30\}$.

Table 4 $\mathbf{SDTS_1 s}$ *for DS VSI CV, DS CV, VP CV and EWMA CV charts for* $\boldsymbol{n_0} \in \{\mathbf{5}, \mathbf{10}, \mathbf{15}\}$, $\boldsymbol{\gamma_0} \in \{\mathbf{0.05}, \mathbf{0.1}\}$ *and* $\boldsymbol{\delta} \in \{\mathbf{1.1}, \mathbf{1.2}, \mathbf{1.5}, \mathbf{2.0}\}$, *based on minimizing* $\mathbf{ATS_1}$ *when* $\mathbf{ATS_0} = \mathbf{370.4}$

n_0	γ_0	δ	DS VSI CV	DS CV	VP CV	EWMA CV
5	0.05	1.1	42.46	55.83 (23.95%)	75.44 (43.72%)	42.33 (-0.30%)
		1.2	12.06	16.58 (27.23%)	20.03 (39.77%)	13.78 (12.45%)
		1.5	2.03	2.97 (31.66%)	4.35 (53.34%)	3.49 (41.84%)
		2.0	0.94	1.26 (25.72%)	1.94 (51.76%)	1.54 (39.23%)
	0.1	1.1	46.37	56.33 (17.68%)	81.85 (43.34%)	42.30 (-9.63%)
		1.2	12.14	16.80 (27.74%)	21.88 (44.52%)	13.87 (12.48%)
		1.5	1.71	3.01 (43.13%)	4.08 (58.04%)	3.55 (51.78%)
		2.0	0.65	1.27 (48.95%)	1.85 (64.96%)	1.57 (58.71%)
10	0.05	1.1	32.24	38.26 (15.74%)	64.81 (50.26%)	22.46 (-43.54%)
		1.2	8.89	9.43 (5.76%)	12.39 (28.27%)	6.74 (-31.86%)
		1.5	0.99	1.31 (24.79%)	2.13 (53.75%)	1.78 (44.65%)
		2.0	0.31	0.47 (34.06%)	1.17 (73.51%)	0.83 (62.66%)
	0.1	1.1	31.28	38.74 (19.27%)	69.48 (54.99%)	22.70 (-37.78%)
		1.2	7.03	9.61 (26.87%)	13.63 (48.44%)	6.84 (-2.74%)
		1.5	0.88	1.34 (34.23%)	1.96 (55.04%)	1.81 (51.31%)
		2.0	0.32	0.47 (32.30%)	1.01 (68.50%)	0.85 (62.56%)
15	0.05	1.1	24.34	31.20 (21.98%)	57.16 (57.41%)	15.70 (-55.05%)
		1.2	4.99	7.04 (29.07%)	9.41 (46.94%)	4.58 (-9.03%)
		1.5	0.58	0.85 (31.34%)	1.48 (60.57%)	1.23 (52.55%)
		2.0	0.21	0.26 (19.77%)	0.93 (77.57%)	0.61 (65.80%)
	0.1	1.1	24.72	31.61 (21.78%)	58.09 (57.44%)	15.93 (-55.20%)
		1.2	5.12	7.18 (28.74%)	9.65 (46.98%)	4.66 (-9.80%)
		1.5	0.60	0.87 (31.47%)	1.50 (60.25%)	1.26 (52.68%)
		2.0	0.21	0.26 (19.54%)	0.94 (77.74%)	0.62 (66.26%)

The novelty of the DS VSI CV chart lies in the integration of two different methods, namely the DS and VSI methods in the development of the new DS VSI CV chart for monitoring the process CV. Prior to this study, only the DS CV chart by Lee et al. [16] exists. Therefore, in this paper, a novel method that leverages on the effectiveness of the VSI method is employed to develop the new DS VSI CV chart to provide a more effective scheme for detecting shifts in the process CV. The superiority of the developed DS VSI CV chart is evident from comparisons of its ATS_1 and SDTS_1 performance with that of existing CV charts in this section, where the former outperforms the latter in detecting small and moderate upward CV shifts. Even though the EWMA CV chart prevails when δ approaches unity, the said chart is plotted using transformed statistics compared with the DS VSI CV chart, whose control charting statistic is plotted on the original scale of measurement. The development of the DS VSI CV chart in this paper provides significant improvement in detecting upward CV shifts and the developed chart can be applied in process monitoring when the standard deviation is proportional to the mean, such as in the monitoring of cyclosporine levels of clinical interest [13], integrated circuit lead electroplating [16], and die casting hot chamber process manufacturing zinc alloy parts for the sanitary sector [18], to name some.

The incorporation of the VSI method into the DS CV chart offers a hybrid framework for designing an adaptive and resource efficient control chart, which enhances the chart's sensitivity to process CV shifts, while minimizing sampling costs. Specifically, the DS VSI CV chart employs a two-phase approach, a preliminary small sample selected for detecting potential deviations, followed by adaptive sampling intervals to expedite the detection of out-of-control conditions. This hybrid strategy improves the detection efficiency of small and moderate CV shifts, as demonstrated by the DS VSI CV chart's ATS_1 performance compared to existing CV charts, discussed in this section. Optimization of the DS VSI CV chart's parameters, such as limits' parameters and sampling intervals,

Int. Journal of Integrated Engineering Vol. 18 No. 3 (2026) p. 118-134

further refine the chart's performance in minimizing ATS_1, ensuring an efficient monitoring across diverse process scenarios.

The shortcomings of the proposed DS VSI CV chart are it is developed based on the assumption that the underlying distribution follows a normal distribution with known process parameters. Hence, the effectiveness of the DS VSI CV chart is compromised when the underlying distribution deviates from normality and the process parameters are unknown. Moreover, the present study requires the assumption that the exact shift size in the process CV can be specified. However, in practice, the exact shift size is usually unknown. Under this situation, the performance of the DS VSI CV chart should be evaluated for an interval of shift sizes by employing an alternative performance measure to assess the efficacy of the chart. The shortcomings of the proposed DS VSI CV chart identified here provide opportunities for further investigations to address the setbacks of the chart.

4. Application of DS VSI CV Control chart

This section demonstrates the implementation of the DS VSI CV chart to monitor the Phase-II process CV. Simulated data obtained using the Statistical Analysis System software are employed for the Phase-I and Phase-II processes. The underlying distribution is based on the assumption that the samples are iid with a normal distribution. The in-control Phase-I data comprise 30 samples, each having n_0 = 5 measurements. The means $\bar{X}_i$, standard deviations S_i and sample CVs $\hat{\gamma}_i$, for i = 1, 2, ..., 30, of these 30 Phase-I samples are shown in Table 5. Here, i denotes the sample number of the Phase-I samples. The in-control CV, $\hat{\gamma}_0$ is calculated using these in-control Phase-I data as $\hat{\gamma}_0 = \sqrt{\frac{[\sum_{i=1}^{30}(n_i-1)\hat{\gamma}_i^2]}{\sum_{i=1}^{30}(n_i-1)}}$, which yields 0.11278 and is rounded to 0.1.

Table 5 *Values of* $\bar{X}$, *S and* $\hat{\gamma}$ *for Phase-I*

i	$\bar{X}_i$	S_i	$\hat{\gamma}_i$
1	10.2587	1.5219	0.1484
2	10.9898	2.0971	0.1908
3	10.6124	1.5968	0.1505
4	10.7974	0.8791	0.0814
5	10.4601	1.0322	0.0987
6	10.1929	0.7435	0.0729
7	8.9837	1.3608	0.1515
8	10.1335	1.3659	0.1348
9	9.8847	0.4874	0.0493
10	10.5271	0.6039	0.0574
11	9.3758	0.6160	0.0657
12	10.4052	0.9431	0.0906
13	10.4282	1.0212	0.0979
14	9.8282	1.5237	0.1550
15	10.0128	0.7664	0.0765
16	9.4580	0.8410	0.0889
17	10.5384	0.9820	0.0932
18	10.0676	0.8101	0.0805
19	10.3196	1.4551	0.1410
20	9.1876	0.9865	0.1074
21	9.9623	0.6867	0.0689
22	10.4294	0.8935	0.0857
23	9.6531	1.4649	0.1518
24	9.6389	1.3010	0.1350
25	10.7171	1.5658	0.1461
26	9.8396	1.2177	0.1238
27	9.6071	0.8450	0.0880
28	9.9757	0.9028	0.0905
29	9.3787	0.7027	0.0749
30	9.2585	1.0922	0.1180

Assume that the shift size $\delta = 1.1$ must be detected quickly. Consequently, from Table 2, it is suggested to use the optimal parameters (n_1, n_2, UCL_1, LCL_1, UWL_2, LWL_2, UCL_2, LCL_2, UWL_1, LWL_1) = (4, 20, 0.2890, 0.0019, 0.1229, 0.0531, 0.1412, 0.0442, 0.1096, 0.0570). These optimal parameters are used to design the DS VSI CV chart, for Phase-II monitoring. The simulated Phase-II dataset consists of 20 sampling points, where n_1 = 4 and n_2 = 20.

The first 10 sampling points are simulated for an in-control process, whereas the last 10 sampling points are simulated based on δ = 1.1 (out-of-control situation). Table 6 shows the summary statistics for the Phase-II dataset, where $\hat{\gamma}_1$ and $\hat{\gamma}^*$ represent the control charting statistics for the first and second sampling stages, respectively.

Table 6 *Phase-II summary statistics for DS VSI CV chart*

Sampling point, i	First sampling stage (n_1 = 4)			Second sampling stage (n_2 = 20)			
	$\bar{X}_1$	S_1	$\hat{\gamma}_1$	$\bar{X}_2$	S_2	$\hat{\gamma}_2$	$\hat{\gamma}^*$
1	10.2438	1.7569	0.1715	10.7064	1.3772	0.1286	0.1353
2	10.4868	0.5722	0.0546				
3	9.8120	0.9434	0.0962				
4	9.1539	1.7956	0.1962	9.9586	0.9079	0.0912	0.1115
5	10.0435	0.9338	0.0930				
6	10.8075	0.6568	0.0607				
7	9.1976	0.6671	0.0725				
8	10.5727	1.3151	0.1244	10.0061	0.9025	0.0902	0.0956
9	10.5059	1.4315	0.1363	9.8809	1.1272	0.1141	0.1174
10	9.8854	2.1406	0.2165	9.8906	0.9357	0.0946	0.1188
11	9.3473	1.7327	0.1854	9.7968	1.3775	0.1406	**0.1475**
12	9.5777	0.5722	0.0597				
13	8.9029	0.9434	0.1060				
14	8.2448	1.7956	0.2178	9.0759	0.8932	0.0984	0.1218
15	9.2143	0.8101	0.0879				
16	9.2401	0.9336	0.1010				
17	8.9400	1.3009	0.1455	9.2220	1.0132	0.1099	0.1154
18	8.5926	0.7618	0.0887				
19	9.7980	1.3768	0.1405	8.8958	1.0664	0.1199	0.1229
20	8.6085	1.4693	0.1707	9.1258	1.1541	0.1265	0.1334

Note: The out-of-control sampling point 11 is denoted by the boldfaced value.

Fig. 2 shows the DS VSI CV chart. At sampling point 1, the $\hat{\gamma}_1$ (= 0.1715) value falls in the interval I_3. Thus, a second sample with n_2 = 20 is taken to calculate $\hat{\gamma}_2$ (= 0.1286) followed by computing the combined sample CV, $\hat{\gamma}^*$ (= 0.1353). Since $\hat{\gamma}^* \in I_4$, an in-control process is obtained (see Table 6 and Fig. 2). The first sample is taken at sampling point 2 after a short sampling interval h_2 (= 0.1). The $\hat{\gamma}_1$ (= 0.0546) value at sampling point 2 plots in I_2, therefore, the second sample need not be taken at sampling point 2. Also, the short sampling interval, h_2 (= 0.1), is used to select the first sample at sampling point 3. At sampling point 3, the $\hat{\gamma}_1$ (= 0.0962) value falls in the interval I_1. Therefore, the second sample need not be taken at sampling point 3. Meanwhile, at sampling point 4, the first sample is selected after a long sampling interval, h_1 (= 1.9). The process of taking samples at each sampling point continues in the same manner until sampling point 11. At sampling point 11, $\hat{\gamma}_1$ (= 0.1854) $\in I_3$, hence, the second sample is taken and $\hat{\gamma}^*$ (= 0.1475) is computed. As this $\hat{\gamma}^* \in I_6$, an out-of-control is signalled at sampling point 11. Hence, remedial actions must be implemented to identify the assignable cause(s), in order to return the out-of-control process to the in-control situation. The remaining sampling points are in-control (see Table 6 and Fig. 2).

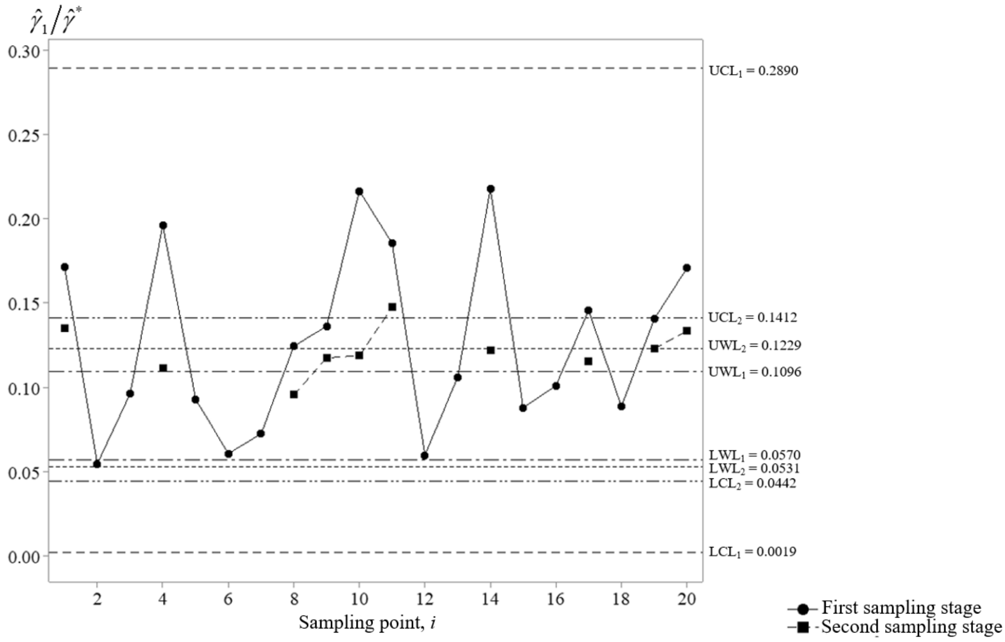

Fig. 2 *DS VSI CV chart for Phase-II monitoring of CV*

5. Conclusion

In certain scenarios, the mean and standard deviation vary in proportion, with the standard deviation to the mean ratio being constant. The said ratio is the CV. Under this condition, controlling process shifts based solely on the mean or standard deviation leads to erroneous judgement about the state of the process. Therefore, monitoring the CV by means of control charts is important. In this paper, the DS VSI CV chart is developed to monitor the CV. In general, the performance comparison in this paper shows that the DS VSI CV chart detects most sizes of CV shifts faster than the existing DS CV, VP CV and EWMA CV charts, in terms of the ATS_1 and $SDTS_1$ performance criteria, except for some small shifts where the EWMA CV chart prevails. The EWMA CV chart has the lowest ATS_1 value when $n_0 \geq 10$ and $\delta = 1.1$, for all γ_0 values. For $SDTS_1$ performance, the EWMA CV chart provides the best performance when $n_0 = 5$ (for $\delta = 1.1$) and $n_0 \in \{10, 15\}$ (for $\delta \in \{1.1, 1.2\}$), for all γ_0 values. Apart from these (n_0, γ_0, δ) combinations, the DS VSI CV chart surpasses the EWMA CV chart. An implementation of the DS VSI CV chart is also provided. The optimal parameters of the DS VSI CV chart are determined to minimize the ATS_1 value, for the shift of size δ. Note that the underlying distribution considered in this study is based on the assumptions of iid samples having the normal distribution with known process parameters. Further research can examine the performance of the DS VSI CV chart when process parameters are estimated and the iid normality assumption is violated. Moreover, in this study, it is assumed that the exact shift size in the process CV can be specified, hence, how the DS VSI CV chart will perform for a range of shift sizes is an interesting research topic which can be studied in a further research.

Acknowledgement

This research was conducted when the corresponding author was spending his sabbatical leave at Estek Automation Sdn Bhd.

Conflict of Interest

Authors declare that there is no conflict of interests regarding the publication of the paper.

Author Contribution

The authors confirm contribution to the paper as follows: data collection, ***data analysis and preparing the draft of the manuscript****: You Huay Woon;* ***methodological development of concepts and ideas, review and checking of the final manuscript****: Michael Khoo Boon Chong;* ***writing of computer programs and checking of the final manuscript****: Sajal Saha;* ***proofreading, improving the English and formatting of the final manuscript****: Yasar Mahmood;* ***proofreading and checking of the final manuscript****: Shanyu Chua. All authors reviewed the results and approved the final version of the manuscript.*

References

[1] Selcem Adsız & Burcu Aytaçoğlu (2023) Tukey-EWMA control chart with variable sampling intervals for process monitoring. Quality Engineering, https://doi.org/10.1080/08982112.2023.2199824

[2] Demetrios L Antzoulakos, konstantinos G Fountoukidis & Athanasios C Rakitzis (2025) The variable sample size and sampling interval run sum Max chart. Quality Technology & Quantitative Management, 22(2), 321–344, https://doi.org/10.1080/16843703.2024.2315837

[3] Maria Eugenia Calzada & Stephen Mark Scariano (2013) A synthetic control chart for the coefficient of variation, Journal of Statistical Computation and Simulation, 83(5), 853–867, https://doi.org/10.1080/00949655.2011.639772

[4] Philippe Castagliola, Achouri Ali, Taleb Hassen, Celano Giovanni & Stelios Psarakis (2013) Monitoring the coefficient of variation using control charts with run rules, Quality Technology & Quantitative Management, 10(1), 75–94, https://doi.org/10.1080/16843703.2013.11673309

[5] Yi Ying Chew, Michael Boon Chong Khoo, Khaw Khai Wah, Lee Ming Ha & Sajal Saha (2025) Optimal designs of variable sample size control chart for monitoring the multivariate coefficient of variation in short production runs, Communications in Statistics - Simulation and Computation, 54(1), 234–251, https://doi.org/10.1080/03610918.2023.2251727

[6] Robert Croasdale (1974) Control charts for a double-sampling scheme based on average production run lengths, International Journal of Production Research, 12(5), 585–592, https://doi.org/10.1080/00207547408919577

[7] Jean-Jacques Daudin (1992) Double sampling $\bar{X}$ charts, Journal of Quality Technology, 24(2), 78–87, https://doi.org/10.1080/00224065.1992.12015231

[8] Sakthiseswari Ganasan, You Huay Woon, Zainol Mustafa & Dadasaheb Ganesh Godase (2023) Memory-type control charts through the lens of cost parameters, Intelligent Automation & Soft Computing, 36, https://doi.org/10.32604/iasc.2023.032062

[9] Eui-Pyo Hong, Kang Chang-Wook, Baek Jae-Won & Kang Hae-Woon (2008) Development of CV control chart using EWMA technique, Journal of Society of Korea Industrial and Systems Engineering, 31(4), 114–120.

[10] Xuelong Hu, Jiening Zhang, Suying Zhang, Panpan Zhou & Yang Zhang (2023) A variable sampling interval one-sided CUSUM control chart for monitoring the multivariate coefficient of variation. Journal of King Saud University - Science, 35(7), 102845. https://doi.org/10.1016/j.jksus.2023.102845

[11] Boris Iglewicz, Raymond Harold Myers, and Richard B Howe (1968) On the percentage points of the sample coefficient of variation, Biometrika, 55(3), 580–581, https://doi.org/10.1093/biomet/55.3.580

[12] Muhammad Imran, Jinsheng Sun, Xuelong Hu, Fatima Sehar Zaidi & Anan Tang (2024). Investigating zero-state and steady-state performance of MEWMA-CoDa control chart using variable sampling interval. Journal of Applied Statistics, 51(5), 913–934. https://doi.org/10.1080/02664763.2023.2170336

[13] Chang Wook Kang, Lee Man S., Seong Young J. & Douglas Michael Hawkins (2007) A control chart for the coefficient of variation, Journal of Quality Technology, 39(2), 151–158, https://doi.org/10.1080/00224065.2007.11917682

[14] Ashari Kasmin, Ibrahim Masood, Nasrull Abdul Rahman, A H Abdul Kadir & Mohd Nasrull Abdol Rahman (2021) Control chart pattern recognition using small window size for identifying bivariate process mean shifts, International Journal of Integrated Engineering, 13(2), 208–213, https://doi.org/10.30880/ijie.2021.13.02.024

[15] Michael Boon Chong Khoo, How Chinh Lee, Zhang Wu, Chung-Ho Chen & Philippe Castagliola (2010) A synthetic double sampling control chart for the process mean, IIE Transactions, 43(1), 23–38, https://doi.org/10.1080/0740817X.2010.491503

[16] Pei-Hsi Lee, Torng Chau-Chen, Jhong Hao-Ren & Chao-Yu Chou (2023) Monitoring the coefficient of variation using a double-sampling control chart, Communications in Statistics - Simulation and Computation, 52(10), 4849–4863, https://doi.org/10.1080/03610918.2021.1971242

[17] Zwelakhe Magagula, Jean-Claude Malela-Majika, Schalk William Human, Philippe Castagliola, Kashinath Chatterjee & Christos Koukouvinos (2025) Closed-form expressions of the run-length distribution of the nonparametric double sampling precedence monitoring scheme, Computational Statistics, 40(1), 273–299, https://doi.org/10.1007/s00180-024-01488-z

[18] Muhammad Noor-ul-Amin & Afshan Riaz (2020) EWMA control chart for coefficient of variation using log-normal transformation under ranked set sampling, Iranian Journal of Science and Technology, Transactions A: Science, 44(1), 155–165, https://doi.org/10.1007/s40995-019-00805-2

[19] Anan Tang, Hu Xuelong, Xie Fupeng & Xiaojian Zhou (2024) Nonparametric adaptive EWMA-type control chart with variable sampling intervals, Communications in Statistics - Simulation and Computation, 53(8), 4001–4017, https://doi.org/10.1080/03610918.2022.2120200

[20] Jing Wei Teoh, Wei Lin Teoh, Zhi Lin Chong, XinYing Chew & Sin Yin Teh (2024) Redesigning the Omnibus SPRT Control chart for simultaneous monitoring of the mean and dispersion of Weibull processes, Int. Journal of Integrated Engineering, 16(5), 201–213, https://doi.org/10.30880/ijie.2024.16.05.016

[21] Wei Lin Teoh, Michael Boon Chong Khoo, Sin Yin Teh, Zhi Lin Chong, Wai Hoong Moy & Huay Woon You (2022) Another look at the VSI EWMA $\bar{X}$ chart when estimating process parameters, International Journal of Electrical and Electronic Engineering & Telecommunications, 11(4), 269–276, https://doi.org/10.18178/ijeetc.11.4.269-276

[22] Shu Wu, Mingyao Tang, Xuelong Hu & JianLan Zhong (2019). Optimal design of the variable sampling interval np control chart for monitoring service process, Procedia CIRP, 83, 242–247.

[23] Wei Yang, Xueting Ji, Hongxing Cai & Jiujun Zhang (2025). Cumulative sum schemes for monitoring the ratio of two correlated normal variables in short production runs with fixed and variable sampling interval strategies: Application in wheat seed processing, Mathematics, 13(4), 657. https://doi.org/10.3390/math13040657

[24] Huay Woon You (2017) Run length distribution of synthetic double sampling chart, International Journal of Applied Engineering Research, 12(24), 14268-14272.

[25] Huay Woon You, Michael Khoo Boon Chong, Chong Zhi Lin & Teoh Wei Lin (2020) The expected average run length of the EWMA median chart with estimated process parameters. Austrian Journal of Statistics, 49(3), 19–24, https://doi.org/10.17713/ajs.v49i3.1020

[26] Huay Woon You, Zhi Lin Chong, Wei Lin Teoh, Michael Boon Chong Khoo & Wai Chung Yeong (2023) An expected average run length (EARL) performance comparison of the SSGR and EWMA control charts, International Journal of Integrated Engineering, 15(5), 35–40, https://doi.org/10.30880/ijie.2023.15.05.005

[27] Huay Woon You, Michael Boon Chong Khoo, Philippe Castagliola & Abdul Haq (2016) Monitoring the coefficient of variation using the side sensitive group runs chart, Quality and Reliability Engineering International, 32(5), 1913–1927, https://doi.org/https://doi.org/10.1002/qre.1922

[28] Ying Zhang, Mengyao Yan & Chuxian Ke (2024). Joint design of VSI Tr control chart and equipment maintenance in high quality process. Journal of Process Control, 136, 103177. https://doi.org/10.1016/j.jprocont.2024.103177

[29] Wenhui Zhou, Zixuan Wang & Wei Xie (2020) Weighted signal-to-noise ratio robust design for a new double sampling npx chart, Computers & Industrial Engineering, 139, 106124, https://doi.org/10.1016/j.cie.2019.106124